XIII Congresso Ibérico de Acústica
55º Congreso Español de Acústica
TECNIACÚSTICA 2024
Faro, 11 a 13 setembro 2024

64-MICROPHONE MODULE FOR A MASSIVE ACOUSTIC CAMERA

Jorge Ortigoso Narro[1], Ricardo Moreno[2]
Daniel de la Prida[3], Marco Raiola[2] and Luis A. Azpicueta-Ruiz[1]

[1]Department of Signal Theory and Communications, Universidad Carlos III de Madrid
{e-mail: jortigos@pa.uc3m.es, lazpicue@ing.uc3m.es}
[2]Department of Aerospace Engineering, Universidad Carlos III de Madrid
{e-mail: jonmoren@ing.uc3m.es, mraiola@ing.uc3m.es}
[3]Department of Audiovisual Engineering and Communications, Universidad Politécnica de Madrid
{e-mail: daniel.prida@upm.es}

Abstract

The recent advancements in micro-electro-mechanical systems (MEMS) technology have opened the opportunity for the reliable use of digital MEMS pressure sensors. Due to these sensors' low power consumption and lightweight design, the trend of instrumentation based on MEMS technology is on the rise. In this paper, we present the design of a scalable low-cost acoustic camera tailored for jet-noise diagnostics. By leveraging MEMS pressure sensors connected in an array configuration, we aim to enhance noise analysis implementing advanced beamforming techniques and allowing the characterization of jet-noise sources from far-field measurements. Intending to render the microphone array both flexible and scalable, the design relies on the use of multiple attachable modules and subsets, enabling easy adjustment and expansion of its dimensions. Every subset comprises a printed circuit board housing 16 sensors, and a microprocessor which is in charge of managing one module of 4 subsets, facilitating the implementation of beamforming techniques. Every module was designed not only to minimize measurement disturbances, but also to reduce its influence in the acoustic field while preserving the overall functionality and reliability of the system.

Keywords: Jet-Noise Diagnostics, Massive Acoustic Camera, Beamforming, MEMS.

PACS nº. 43.60.Fg, 43.20.Ye

1 Introduction

Phased microphone arrays have been developed over the last fifty years as an instrument to localize sources emitting sound [1], mimicking the radar process to estimate the position of an object by the joint analysis of simultaneous signals. This technology provides an alternative method to assess sound emission by identifying and localizing sources with the highest sound energy contribution. Furthermore, moving objects like aircraft, trains, cars, and other machinery can be analyzed to diagnose the acoustic emission of those parts or components that emanates the most significant sound contribution. [2]. The use of acoustic cameras has been on the rise due to their flexibility and ability to capture sound contributions under difficult scenarios. Based on inverse models of sound propagation and arrival estimation, other noise contributions are separated from the desired acoustic signals, such as speech data acquisition systems, audio surveillance, and static sound sources detection [3, 4].

In outdoor environments, the primary energy contributions from a complex group of noise sources can be localized by using this instrument. Whereas, in more controlled conditions, noise diagnostics are obtained, enabling the study of the acoustic emissions produced by physical phenomena with object interactions. Indeed, identifying where the sound generation is happening is crucial for acoustic design

and noise emission optimization [5]. This tool allows for an effective noise reduction, by applying noise mitigation strategies to those identified sub-sources that contribute the most to the overall sound pressure levels.

In practice, the localization capability of microphone arrays is constrained by the number of microphones and separation between them. At low frequencies, the acoustic localization is limited by the end to end distance of the microphone array, since a larger microphone array aperture is needed to capture longer wavelengths. This issue represents a challenge for finding a compromise between the size of the array and the number of sensors. At high frequencies, spatial aliasing occurs, which is tightly related to the array's directivity. This type of aliasing appears for those frequencies with wavelengths shorter than half the distance between the microphones, leading to inaccurate sound localization [2]. These issues can be solved by building bigger arrays with a vast number of microphones, yet increasing the number of transducers to acquire acoustic signals means rising the price of the measurement system and its computational cost. In this sense, Micro-Electro-Mechanical Systems (MEMS) are preferred for acoustic and vibroacoustic measurements for their price, dimensions, and integrated digital signal conditioning. The employment of MEMS technology has led to the possibility to build low-cost and precise instrumentation with less electronic complexity. To illustrate, Pankaj's proposed array [6] employs a 16 MEMS microphone group, which showed strong qualitative results as well as quantitative agreement in comparison to an array of precision condenser microphones. This methodology demonstrates that lower-cost MEMS sensor systems can be achievable, reliable, and, at times, comparable with a class 1 microphone array. Other MEMS-based arrays have been proposed in [6–8] with the goal of providing low-cost and low-power measurement systems. However, most of the previous approaches, while achieving affordable array platforms, were not designed for either being part of a large-scale array of transducers creating a massive acoustic camera nor for being employed for far-field jet-noise studies.

Hence, the prototype proposed in this work is focused to diagnose and characterize the sound coming from a cold air jet facility [9], where microphones will be placed in parallel to the streamwise axis. Through this measurement technique, noise source generated by turbulent airflow produced by jet engines can be studied and characterized with an optimized design. These diagnostics capabilities can drive the design of more silent jet engines, modifying the flow to suppress the most acoustically annoying flow fluctuations.

The design criteria of this acoustic camera are based on an electronically optimized modular system, with low-cost components. To achieve this, three main aspects have been considered: (1) the ability to measure jet noise, (2) the capacity to shape-shift the group of subarrays and (3) the possibility of scaling up to a larger acquisition system. For jet noise studies, the design of the microphone array must span the most relevant sections of the jet in the streamwise direction. Next, the configuration of the subarrays must be flexible to be square or rectangular, covering the jet plume regions. Another potential enhancement to the resolution of the results is the scalability of the number of microphones and array dimensions. Finally, the selected microphones not only allow for optimized digital audio conversions, but also microprocessor use a high-speed data traffic interface to send the audio to a master data collector, allowing for the construction of a massive acoustic camera with 1024 sensors. This feature is desirable for attaching more subarrays identical to this.

The design of the microphone array is evaluated by simulating its acoustic response, considering physical properties and microphone distribution. The capability of the beamforming prototype is demonstrated by using the delay-and-sum algorithm with a spherical sound source propagation model, considering the microphone positions and different source locations. As a result, the size of the array and distance between microphones leads to a limitation of the directivity and spatial aliasing.

The remainder of this communication is organized as follows. In Section 2, details and design criteria are explained. Next, the methodology under which the prototype was evaluated is presented in Section 3. Conclusions are shown in Section 4.

2 Acquisition System

This initial phase of project involves designing the hardware capable of measuring acoustic waves using a large number of microphones while keeping the cost low. Additionally, the scalability of the arrays, which consists of connecting multiple identical acquisition modules in parallel, requires efficient data

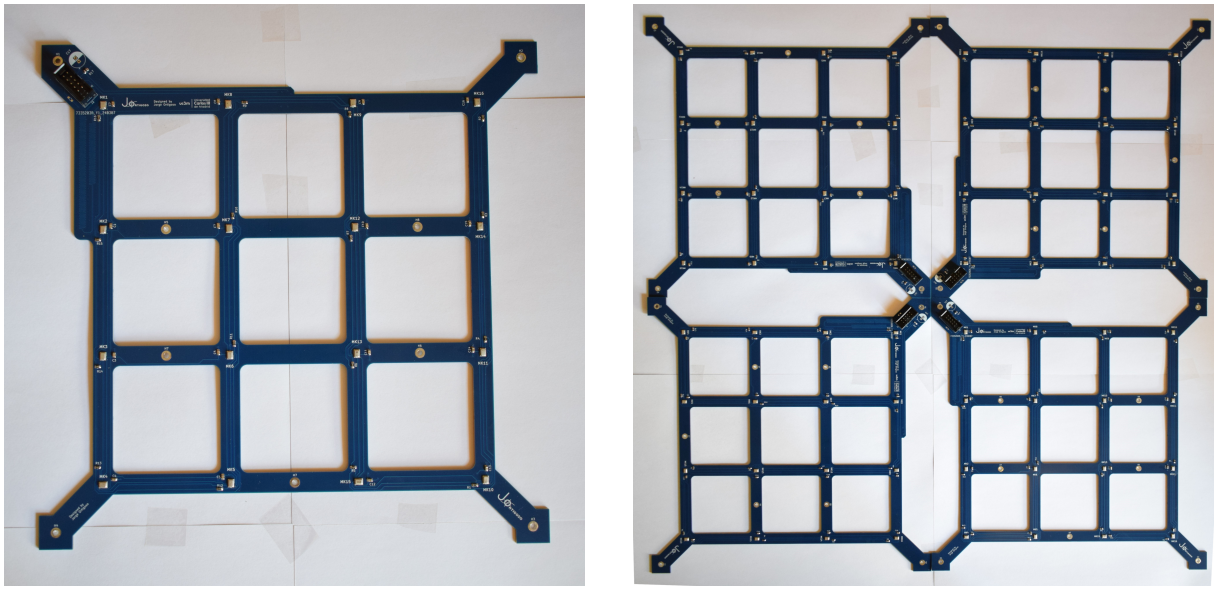

Figure 1 – Left shows a 16 microphone sub-module PCB. Right shows the complete 64 microphone module comprised of four 16 microphone sub-modules.

traffic management.

2.1 Concept design

To characterize the sound source position in terms of its elevation and azimuth, a bi-dimensional distribution of sensors is needed, which leads to an increase in both cost and complexity. In our design we opted to use a Uniform Planar Array (UPA) with the microphones placed in a square grid, see Figure 1. This allows for easier geometrical scalability since growing the size of the array while maintaining the spatial pattern is straightforward.

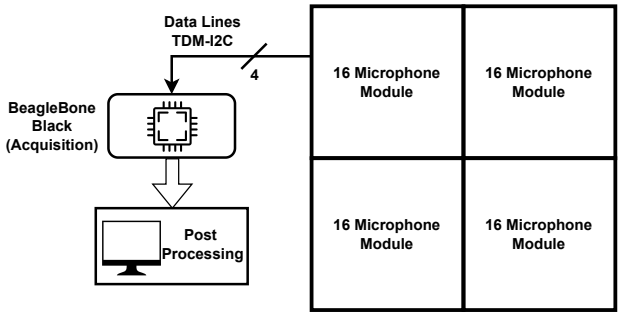

Figure 2 – Concept diagram for the array configuration and data acquisition strategy.

Following [6] we decided to employ smaller 16-microphone sub-modules to allow for more flexibility in the acquisition strategy and in the array configuration. Figure 2 shows the concept diagram.

2.2 Acquisition strategy and data transmission

The vast quantity of data generated by microphone arrays requires advanced signal acquisition and processing strategies. To harness the full potential of these arrays, particularly for applications like beamforming, all elements should capture sound simultaneously to enable for precise phase alignment

of the signals.

With this in mind, we chose the ICS-52000 MEMS microphone for several reasons. Firstly, its design is specifically tailored for array applications, providing an efficient multiplexing interface. Additionally, its output is already digitized, which eliminates the signals' path noise effect on the acquired signal. The ICS-52000 also boasts a scalable easy-to-use data interface such as I^2C with time domain multiplexing (TDM) while maintaining exceptionally low-cost, remarkable signal to noise ratio and frequency response. These microphones allow for a daisy-chained style connection where the clock and data lines are common for every sensor and the sampling is done sequentially throughout all of the chain. Each sub-module is fed by its microprocessor (see Figure 2) with a clock with 24.5 MHz which allows us, with ease, to acquire the signal of the microphones sampled at 48 kHz, to acquire data from the four sub-modules that comprise the 64 microphone array, we employ a BeagleBone Black development platform since it features up to four full-speed I^2C interfaces. Figure 3 (right) shows the interface connections inside a 16-microphone sub-module.

2.3 Hardware design

Each printed circuit board (PCB) was designed to accommodate 16 MEMS pressure sensors, spaced equally from each other and positioned halfway between the board's edge to maintain consistent spacing when integrating more modules. The designs were done following the sensor manufacturer recommendations to ensure signal integrity and to minimize propagation delay mismatches, as well as to reduce the impact of the system's presence in the measurement field.

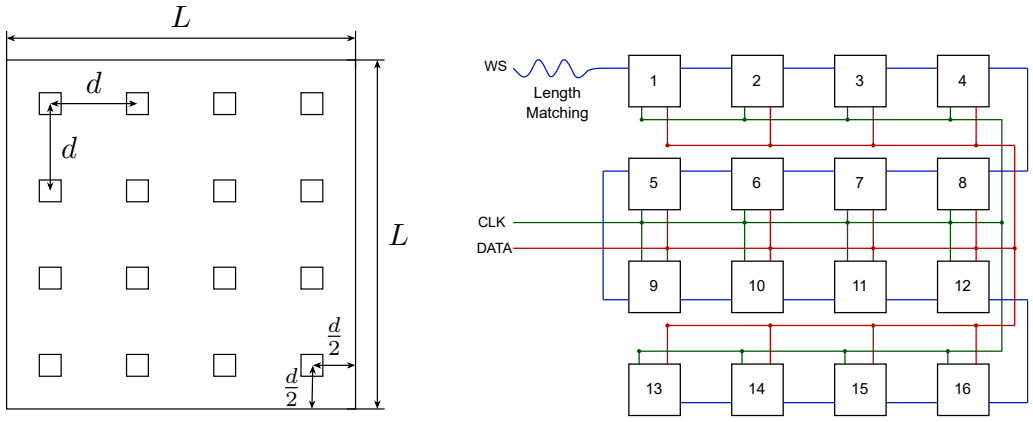

Figure 3 – The diagram on the left shows the 16 microphone sub-module array geometry, where the selected configuration is $L = 25$ cm and $d = 62.5$ mm. The diagram on the right shows the MEMS electrical connections.

To avoid ringing, all the digital traces — clock (CLK), serial data (DATA), and chip/word-select (WS) — were designed to have 50 Ω impedance. A 20 Ω terminating resistor was placed close to each microphone's data bus pin to prevent impedance mismatches between the copper trace and the MEMS chip, which might cause distortion of the signal waveform and compromise the accuracy of the sensor readings. With the aim of reducing the propagation delay, the high-speed lines were connected to the middle of the daisy chain, effectively halving the maximum delay by cutting the trace length in half. Since the word-select line starts in the first microphone of the chain, its length was increased to match the delay introduced by the difference in distance to the connector. Additionally, a minimum spacing equal to the trace width was kept between each line to minimize cross-talk [10]. Figure 3 (right) depicts the onboard electronic connections of the sensors.

Instead of following the approach suggested in [6], we made the decision not to add a buffer driver in order to simplify the electronics connections. The decision was supported by the following considerations:

- Given a medium of $\varepsilon = 4.6$ (FR-4), a 24.5 MHz clock has a wavelength of 5.7 m. By taking a conservative approach, a distance of $\lambda/20$ can be used as a maximum to decide if buffering is needed [11].

- Tri-state capacitance for each sensor is reported to be around 6 pF per microphone. Taking into account the series resistance matching and the line capacitance, the total value is approximately 96 pF, which is considerably under the maximum capacitive load of 150 pF for a 2 ns propagation delay.

2.3.1 Mechanical design

In terms of mechanical design, we opted for a square-shaped design of 25 cm × 25 cm for each 16 microphone sub-module to host the microphones in a grid, easing the expansion with additional modules. To improve the manufacturability and the mechanical strength of the board we chose a 4 layer stack up, which allows for smaller controlled impedance traces and a reduction in the risk of array's curvature or bend due to temperature changes.

To minimize the impact of the systems' presence in the measuring environment, the PCB was designed to have as much hollow space as possible without compromising the mechanical integrity of the board. The holes throughout the surface of the PCB allow the pressure wave to reach the sensor with less delay, which also helps with the diffraction needed for the omnidirectionality of the microphones. This also serves to minimize reflections on the surface of the board, whose influence will be measured in an anechoic chamber.

3 Beamforming Performance

To ensure the correct operation of the electronics and as a test of the viability of the prototype, the fixed distance between microphones was set to 62.5 mm. Indeed, microphone separation determines the capability of the array to acquire high frequencies without grating lobes produced by spatial aliasing [12]. This sets the maximum aperture while maximizing the number of microphones, since the total length of the data line was recommended to be around 50.8 cm to match the maximum delay supported by the data interface. Consequently, the aperture, i.e. the distance between end-to-end microphones, defines the low-frequency acquisition capability.

The classic sensors array literature [13] often presents only the planar wave model, either for near or far-field applications. The planar waves method is unable to identify the position of the source in the far-field, but the direction or incidence angles can be determined in both near and far-field. In recent works [14], the distance calculation applied is equivalent to the propagation of a spherical wave model, resulting in useful also for larger normal distances. To allow for a better characterization, we employed this latter method in our design procedure. Figure 4 shows the simulation results for the frequency with better response (4843 Hz) and for the frequency corresponding to treating the microphone separation as half-wavelength (2744 Hz). For frequencies with a wavelength higher than $\lambda = d = 62.5$ mm spatial aliasing starts to occur for $f \gtrapprox 5.5$ kHz as can be seen in the left plot of Figure 4, where secondary high-level lobes start to appear.

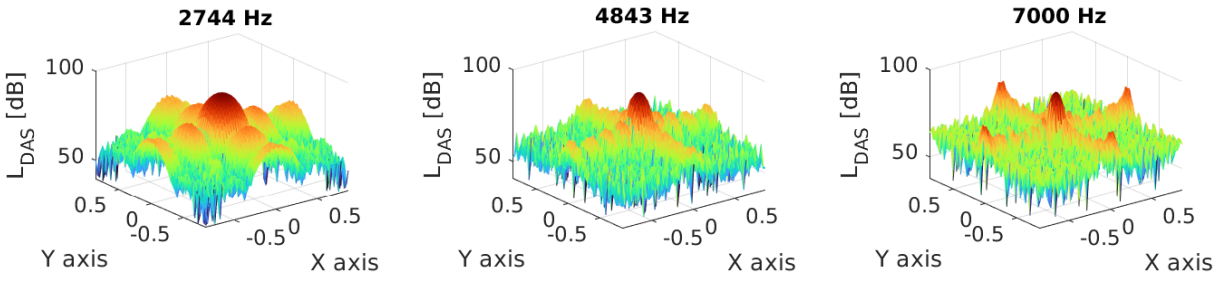

Figure 4 – Spherical wavefront response for broadside direction ($\phi = \theta = 0$) and a range of 1m from the punctual source emitting 1 Pa. Delay and Sum algorithm was used to collect the incident wave. Beamwidth@-3 dB for $f = 2744$ Hz is 232 mm and for $f = 4843$ Hz is 131 mm.

Due to the spherical propagation model, a change in range affects the array behavior since the wavefront gets progressively more planar, Figure 5 (right) shows how the response pattern is affected by the distance

to the source for 4843 Hz.

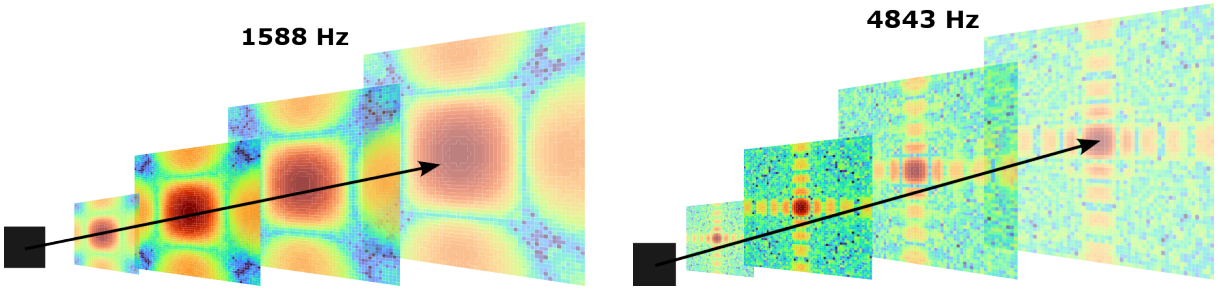

Figure 5 – Left shows spherical wavefront response for broadside direction ($\phi = \theta = 0$) and different ranges for $f = 1588$ Hz. Right shows the spherical wavefront response for broadside direction and different ranges for $f = 4843$ Hz. The black square represents the microphone array.

The array's aperture represents a limitation regarding the lowest frequency to acquire, this can bee seen in Figure 5 (left), where the frequency with wavelength equal to half the aperture of the array (1588 Hz) presents a wider beam than the one in Figure 5 (right). To capture changes in lower frequencies accurately, larger arrays are needed to cover the wavelength of the incident signal.

4 Conclusions and Future Research Directions

This work addresses the design process of a microphone module for a massive acoustic camera tailored for jet-noise experiments for far-field and controlled conditions. The proposed design leverages from MEMS pressure sensors to provide accurate measurements while maintaining both low-cost and great scalability.

Each 64-microphone module is arranged by adding four smaller 16-microphone sub-modules. Microphones are placed on a square grid, allowing for easier geometrical scalability by simplifying the sensors' distribution. Providing an easy solution to increase the number of microphones allows for a more flexible acquisition strategy and configuration. Simulations were carried out to analyze the array's response to a spherical wavefront in terms of lobular pattern and beam width. The highest frequencies that can be accurately captured are restricted by the phenomenon of spatial aliasing, which starts to occur for frequencies with wavelength smaller than 62.5 mm, which corresponds to the distance between microphones. Therefore, the limit for spatial aliasing of this prototype is 5.5 kHz. Additionally, the physical aperture of the array imposes a lower limit on the frequencies that can be effectively measured. Frequencies below this threshold may not be captured with sufficient accuracy, leading to potential loss of information. For the 64-microphone module, the minimum frequency is 784 Hz approximately. By making the system scalable, the lower bound can be improved since the aperture would be increased by creating a bigger surface array by joining multiple modules.

To characterize the acquisition system, measurements within an anechoic chamber will be carried out to evaluate the array limitations in its ability for spatial discrimination in terms of both beam width and range, as well as the effects in the limits due to spatial aliasing. The effect of the presence of the array in the acoustic field will also be evaluated.

Acknowledgements

This activity is part of the project JAMAICAM (Grant No TED2021-130909A-I0), funded by MCIN/AEI/ 10.13039/501100011033 and by the "European Union NextGenerationEU/PRTR". Additionally, the work of D. de la Prida and L. A. Azpicueta-Ruiz was also partly supported by Grant PID2021-124280OB-C21, funded by MCIN/AEI/ 10.13039/501100011033 and by the "ERDF A way of making Europe" funds.

References

[1] J. Billingsley and R. Kinns, "The acoustic telescope," *Journal of Sound and Vibration*, vol. 48, no. 4, pp. 485–510, Oct. 1976. [Online]. Available: https://www.sciencedirect.com/science/article/pii/0022460X76905526

[2] U. Michel, "HISTORY OF ACOUSTIC BEAMFORMING," 2006.

[3] J. Busset, F. Perrodin, P. Wellig, B. Ott, K. Heutschi, T. Rühl, and T. Nussbaumer, "Detection and tracking of drones using advanced acoustic cameras," 10 2015, p. 96470F.

[4] A. Lorenc, D. Król, and K. Klessa, "An acoustic camera approach to studying nasality in speech: The case of Polish nasalized vowels," *The Journal of the Acoustical Society of America*, vol. 144, no. 6, pp. 3603–3617, 12 2018. [Online]. Available: https://doi.org/10.1121/1.5084038

[5] F. Casagrande Hirono, A. Torija, and A. Elliott, "Optimization of a contra-rotating propeller rig for reduced psychoacoustic impact," *INTER-NOISE and NOISE-CON Congress and Conference Proceedings*, vol. 265, pp. 4077–4087, 02 2023.

[6] P. Joshi, F. Khelfa, H. Lehmkuhl, P. Cordes, P. Naujoks, T. Scharowsky, and K. Kochan, "Design, development and testing of digital MEMS pressure sensor array for full-scale vibroacoustic measurements," *INTER-NOISE and NOISE-CON Congress and Conference Proceedings*, vol. 263, no. 2, pp. 4343–4354, Aug. 2021.

[7] A. Izquierdo, J. J. Villacorta, L. Del Val Puente, and L. Suárez, "Design and Evaluation of a Scalable and Reconfigurable Multi-Platform System for Acoustic Imaging," *Sensors*, vol. 16, no. 10, p. 1671, Oct. 2016, number: 10 Publisher: Multidisciplinary Digital Publishing Institute. [Online]. Available: https://www.mdpi.com/1424-8220/16/10/1671

[8] B. da Silva, L. Segers, A. Braeken, K. Steenhaut, and A. Touhafi, "A low-power fpga-based architecture for microphone arrays in wireless sensor networks," in *Applied Reconfigurable Computing. Architectures, Tools, and Applications*, N. Voros, M. Huebner, G. Keramidas, D. Goehringer, C. Antonopoulos, and P. C. Diniz, Eds. Cham: Springer International Publishing, 2018, pp. 281–293.

[9] J. R. Moreno, L. Franceschelli, D. De la Prida, L. A. Azpicueta-Ruiz, and M. Raiola, "Implementation of a Jet Collector and Dissipation Cavity into a Closed Anechoic Chamber for Jet Noise Studies," in *30th AIAA/CEAS Aeroacoustics Conference (2024)*, ser. Aeroacoustics Conferences. American Institute of Aeronautics and Astronautics, May 2024. [Online]. Available: https://arc.aiaa.org/doi/10.2514/6.2024-3066

[10] F. D. Mbairi, W. P. Siebert, and H. Hesselbom, "High-frequency transmission lines crosstalk reduction using spacing rules," *IEEE Transactions on Components and Packaging Technologies*, vol. 31, no. 3, pp. 601–610, 2008.

[11] A. Djordjevic, R. Biljie, V. Likar-Smiljanic, and T. Sarkar, "Wideband frequency-domain characterization of FR-4 and time-domain causality," *IEEE Transactions on Electromagnetic Compatibility*, vol. 43, no. 4, pp. 662–667, Nov. 2001. [Online]. Available: https://ieeexplore.ieee.org/document/974647

[12] J. Benesty, M. M. Sondhi, and Y. A. Huang, Eds., *Springer Handbook of Speech Processing*, ser. Springer Handbooks. Berlin, Heidelberg: Springer, 2008. [Online]. Available: http://link.springer.com/10.1007/978-3-540-49127-9

[13] J. Benesty, M. M. Sondhi, and Y. Huang, *Springer Handbook of Speech Processing*. Springer Science & Business Media, Nov. 2007, google-Books-ID: Slg10ekZBkAC.

[14] O. Jaeckel, "STRENGTHS AND WEAKNESSES OF CALCULATING BEAMFORMING IN THE TIME DOMAIN."